



Design of a PID-PSS Power System Stabilizer for Single-Machine Infinite-Bus Power System

Mehdi Mahdavian ^{*1}, Ali Asghar Amini ^{2,3}, and Mahnaz Hashemi ^{2,3}

¹ Department of Electrical Engineering, Naein Branch, Islamic Azad University, Naein, Isfahan, Iran.

² Department of Electrical Engineering, Najafabad Branch, Islamic Azad University, Najafabad, Iran.

³ Smart Microgrid Research Center, Najafabad Branch, Islamic Azad University, Najafabad, Iran.

Received: 27-Oct-2021, Revised: 15-Dec-2021, Accepted: 20-Jan-2022.

Abstract

Power system stabilizer (PSS) generates electrical torques by applying a signal to the excitation system, which reduces power oscillations. The PSS's main function is to damp generator rotor oscillations. In this paper, the structure of a PSS based on PID controller for system stability enhancement is presented. The voltage regulator excitation system is equipped with IEEE type-DC1 exciter model. The application of the controller is investigated by means of simulation studies on a single machine infinite bus power system. For the system without any PSS and the system with conventional PSS (CPSS) and proportional-integral-derivative PSS (PID-PSS), the system responses for three different conditions were obtained using equations linear simulation. Eigenvalue analysis is used for comparison. The simulation results show that the controller is effective in improving steady state and dynamic performances regardless of the system operating conditions.

Keywords: Power System Stabilizer, Single-Machine Infinite-Bus (SMIB), PID controller.

1. INTRODUCTION

Power System Stabilizer (PSS) is a feedback controller (part of a synchronous generator

control system), which provides an additional signal, which is added to the input sum point in the automatic voltage regulator [1,2].

PSS provides a positive contribution by damping the oscillations of the generator

*Corresponding Authors Email:
meh_mahdavian@yahoo.com

rotor angle that are present in a wide range of frequencies in the power system [3,4].

These range from low frequency inertie modes (typically 0.1-1.0 Hz), to local modes (typically 1-2Hz), to intra-plant modes (about 2 -3 Hz). Therefore, power system stabilizers are mostly used to eliminate system oscillations as well as to increase the damping of electromechanical modes [5,6].

Various studies on the use of PSS have been performed to improve or increase the stability of the power system [7,8]. A number of papers have suggested the simultaneous use of PSS with FACTS devices to improve power system performance [9,10]. Stabilizers have also been used in energy systems to improve system performance [11,12].

The PID controller has a simple structure and is easy to design, so it is widely used in many industrial applications [13,14]. Various studies have been performed on the use of this controller and PSS. A self-tuning PID-PSS based on a decentralized structure for improving the dynamic stability of a multi-machine power system over a wide range of operating conditions is presented in [15], which only local measurements within each generating units are required for the adaptation process.

The optimal design of settings of PSS parameters that shifts the system eigenvalues associated with the electromechanical modes to the left in the s-plane using evolutionary programming optimization technique is presented in [16].

A PSS based on fractional order PID controller hybridization and PSS for optimal stabilization, using the meta-heuristic optimization algorithm in [17] is proposed, which has been tested on an SMIB power

system under various malfunctions and operating conditions.

To minimize low-frequency oscillations in a power system, an interval type-2 fractional order fuzzy proportional integral derivative-PSS is proposed in [18], where speed deviation and acceleration are considered as input signals. Also, a hybrid firefly algorithm-particle swarm optimization scheme for optimizing the parameters is used.

An optimal method for designing a robust PID-PSS is proposed in [19], which uses an interval arithmetic to an optimum PID-PSS to improve the performance of a SMIB system.

The objective of this paper is to investigate the effects of PSS based PID controllers on power system electromechanical oscillation damping. The synchronous generator is represented by the third-order model. The parameters of PSS are determined based on a linearized model of the power system around a nominal operating point where they can provide good performance. The effectiveness of the proposed PSS in increasing the damping of low-frequency oscillation is demonstrated in a SMIB for different operating conditions of the power system.

2. POWER SYSTEM DYNAMIC MODEL

The SMIB power system configuration shown in Fig. 1 with IEEE type-DC1 excitation system is considered for this study. It consists of a shunt load in bus T and impedance of the transmission line. U_T and U_B are the terminal voltage and infinite-bus voltage respectively.

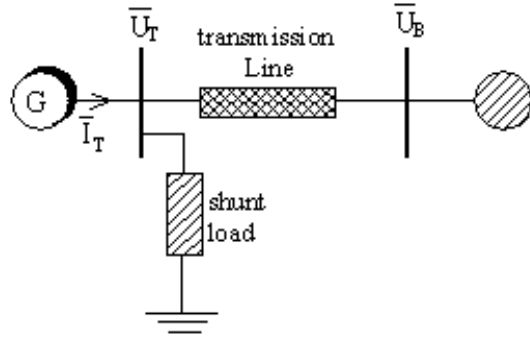


Fig. 1. Single-Machine Infinite-Bus Power System.

2.1. Synchronous Machine

Synchronous machines are predominantly used in power generation. A synchronous machine is a doubly excited machine. The three-order model of synchronous machine is used to design a PSS controller. The non-linear dynamic model of the generator is given by [20,21]:

$$\frac{d}{dt} \delta = \omega_b \omega_r \quad (1)$$

$$\frac{d}{dt} \omega_r = \frac{1}{J_M} (T_M - T_E) \quad (2)$$

$$\frac{d}{dt} E'_q = \frac{1}{T_{do}} [E_F - E'_q + (X'_d - X_d) i_d] \quad (3)$$

2.2. Excitation System

Good design of excitation systems provides operational reliability, stability and fast transient response. The basic function of an excitation system is to provide a continuous current to the field winding of a synchronous machine [22]. The exciter model used in this study is the standard IEEE type-DC1 exciter [23]. The exciter transfer function between the electrical field voltage deviation (ΔE_F) and the error voltage deviation (ΔU_E) of the

excitation system as shown in Fig. 2 is given by [24]:

$$\begin{aligned} G_V(s) &= \frac{\Delta E_F(s)}{\Delta U_E(s)} \\ &= \frac{G_U(s)G_A(s)}{1 + G_S(s)G_U(s)G_A(s)} \end{aligned} \quad (4)$$

where $G_A(s)$, $G_S(s)$ and $G_U(s)$ are transfer functions of the voltage regulator system, excitation system stabilizers and saturation. U_E is the voltage error. K_A , K_E and K_S are gains and T_A , T_E and T_S are time constants of the system exciter. Bode plot of the exciter for two different cases include IEEE Type-DC1 exciter system with transfer function $G_V(s)$ and IEEE Type-ST1 exciter system with transfer function $G_A(s)$ are shown in Fig. 3.

2.3. Synchronizing and Damping Torque

The electric torque has two components: damping torque (in phase with speed) and synchronizing torque (in phase with power angle). The change in the electrical torque deviation can be expressed in terms of reference voltage and rotor angle deviations:

$$\begin{aligned} \Delta T_E(s) &= K_1 \Delta \delta + K_2 \Delta E'_q(s) \\ &= K_1 \Delta \delta + \underbrace{\frac{-K_2 G_F(s) [K_4 + K_5 G_V(s)]}{1 + K_6 G_F(s) G_V(s)}}_{H_Q(s)} \Delta \delta \\ &\quad + \underbrace{\frac{K_2 G_F(s) G_V(s)}{1 + K_6 G_F(s) G_V(s)}}_{G_E(s)} \Delta U_R(s) \end{aligned} \quad (5)$$

where $H_Q(s)$ is the control transfer function (between the electrical output torque and load angle) and $G_E(s)$ is the electrical loop transfer function (between exciter input and the output electrical torque).

The synchronizing torque (T_s) and damping torque (T_d) coefficients are defined as:

$$T_s(\omega) = \text{Re}[H_Q(j\omega)] + K_1 \quad (6)$$

$$T_d(\omega) = \frac{\omega_b}{\omega} \text{Im}[H_Q(j\omega)] \quad (7)$$

They are sensitive to power system parameters, synchronous generator operating conditions, and excitation control system parameters.

2.4. Conventional Lead-Lag PSS

Electromechanical oscillations of power system are damped by compensator as shown in Fig. 4. The gain and the lead-lag compensator time constants are to be selected for optimal performance over a wide range of operating conditions. The transfer function of CPSS is given by [25,26]:

$$G_L(s) = K_C \frac{T_W s}{1+T_W s} \left(\frac{1+T_D s}{1+T_G s} \right)^2 \quad (8)$$

2.5. PID-PSS

A PID controller is commonly used by industrial utilities [27,28]. It can be represented in transfer function form as [29,30]:

$$G_C(s) = K_P + \frac{K_I}{s} + K_D s \quad (9)$$

where K_P represents the proportional gain, K_I represents the integral gain, and K_D represents the derivative gain, respectively. The phase angle diagram of the PID controllers for different values of gains are shown in Fig. 5. The PID-PSS as shown in Fig. 6 with rotor deviation as input have the following transfer function [31]:

$$G_P(s) = K_G \left(\frac{T_W}{1+T_W s} \right) \left(K_P + \frac{K_I}{s} + K_D s \right) \quad (10)$$

The corresponding magnitude and phase characteristics are given by:

$$M(\omega) = K_G \frac{T_W}{\sqrt{1+(T_W \omega)^2}} \sqrt{K_P^2 + \left(K_D \omega - \frac{K_I}{\omega} \right)^2} \quad (11)$$

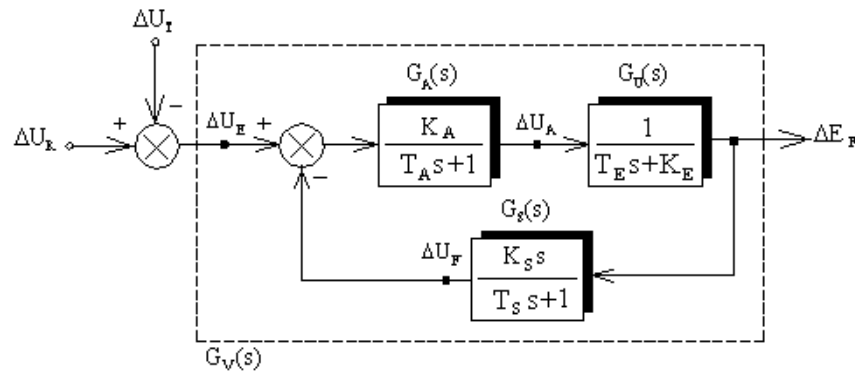


Fig. 2. IEEE type-DC1 excitation system.

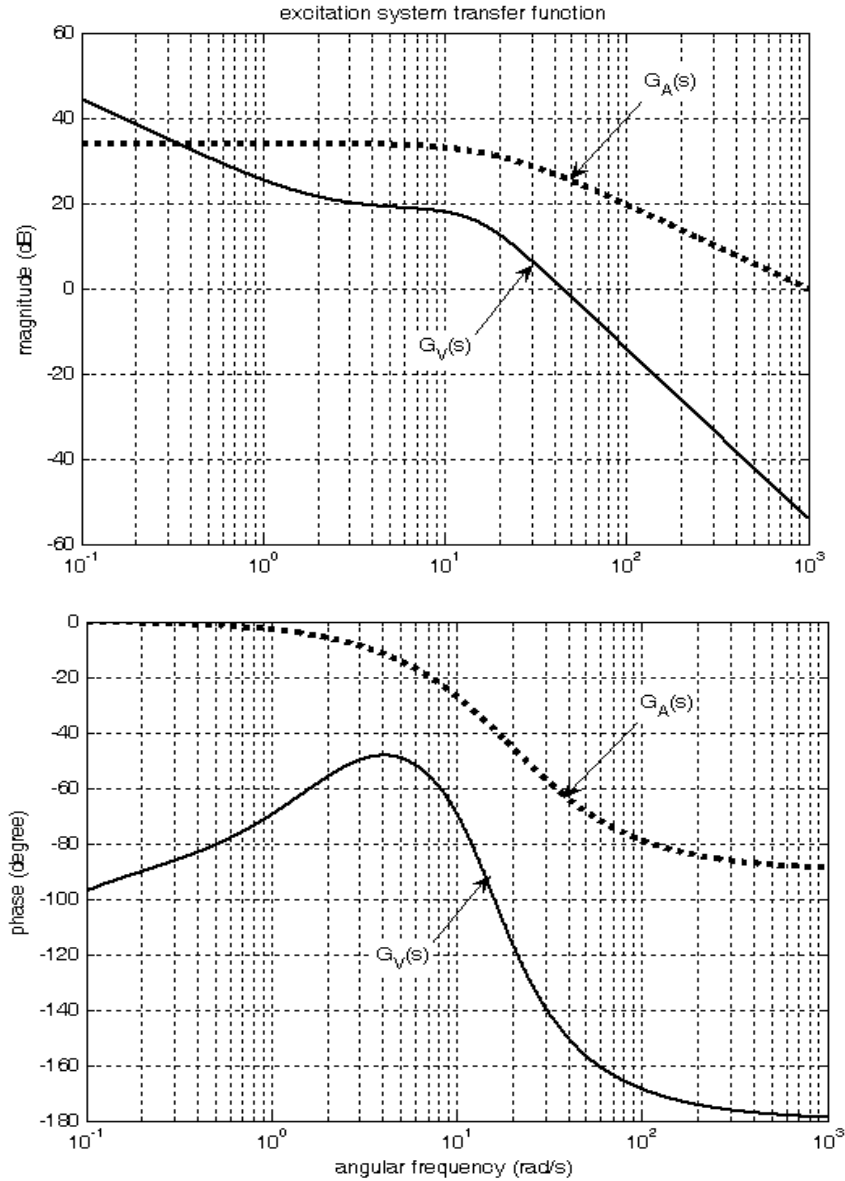


Fig. 3. Bode plot of transfer function $G_V(s)$.

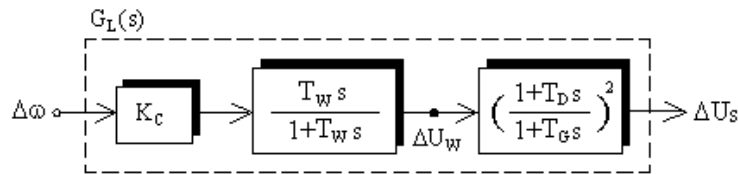


Fig. 4. Block diagram of conventional power system stabilizer (CPSS).

$$\theta_p(\omega) = 180$$

$$+ \text{tg}^{-1} \frac{[K_P - T_W(K_I - K_D\omega^2)]\omega}{K_I + (K_P T_W - K_D)\omega^2} \quad (12)$$

2.6. Transfer Function

The transfer function block diagram representing the small signal stability model can be

simplified as shown in Fig. 7. The linearized model of a SMIB power system has six eigenvalues. Therefore, the characteristic equation of the open loop SMIB power system is given by:

$$\Delta_T(s) = s^6 + g_5s^5 + g_4s^4 + g_3s^3 + g_2s^2 + g_1s + g_0 \quad (13)$$

By varying the operating point, the coefficient parameter values g_0 through g_5 also vary. The open loop transfer function from $\Delta\omega_r$ to ΔU_R , which plays an important role in the closed loop design, is given by:

$$H_{SU}(s) = \frac{\Delta\omega_r(s)}{\Delta U_R(s)} = \frac{sG_M(s)G_E(s)}{s + \omega_b G_M(s)[K_1 + H_Q(s)]} \quad (14)$$

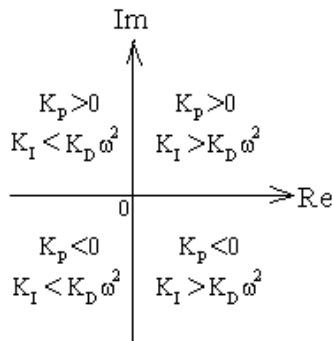


Fig. 5. Phase angle diagram of the PID controller.

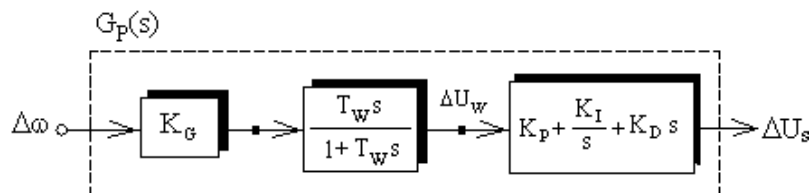


Fig. 6. Block diagram of PID power system stabilizer (PID-PSS).

$$H_{SU}(s) = \frac{\Delta\omega_r(s)}{\Delta U_R(s)} = \frac{1}{\Delta_T(s)} \left(-\frac{K_2 K_A}{\underbrace{J_M T_{do}' T_E T_A}_{K_o}} \right) s \left(s + \frac{1}{T_S} \right) \quad (14)$$

3. SMALL SIGNAL MODEL

Small signal stability is best analyzed by linearizing the system differential equations about equilibrium operating point. Fig. 8 displays a block diagram of a SMIB comprehensive model. The linearized model parameters K_1 to K_6 vary with operating point (P_{EO} , Q_{EO} , U_{TO}) with the exception of K_3 . The synchronous machine model along with the associated regulating devices thus becomes an eight-order model for PID-PSS and nine-order model for CPSS. When the PSS is used in a SMIB power system, the closed loop transfer function can be expressed as follows:

$$H_{RU}(s) = \frac{\Delta\omega_r(s)}{\Delta U_R(s)} = \frac{H_{SU}(s)}{1 - H_{SU}(s)G_P(s)} \quad (15)$$

By using $H_{RU}(s)$, the characteristic equation of the closed loop SMIB power system equipped with PID-PSS is given by:

$$\Delta_{HP}(s) = s(s^7 + h_6s^6 + h_5s^5 + h_4s^4 + h_3s^3 + h_2s^2 + h_1s + h_0) \quad (16)$$

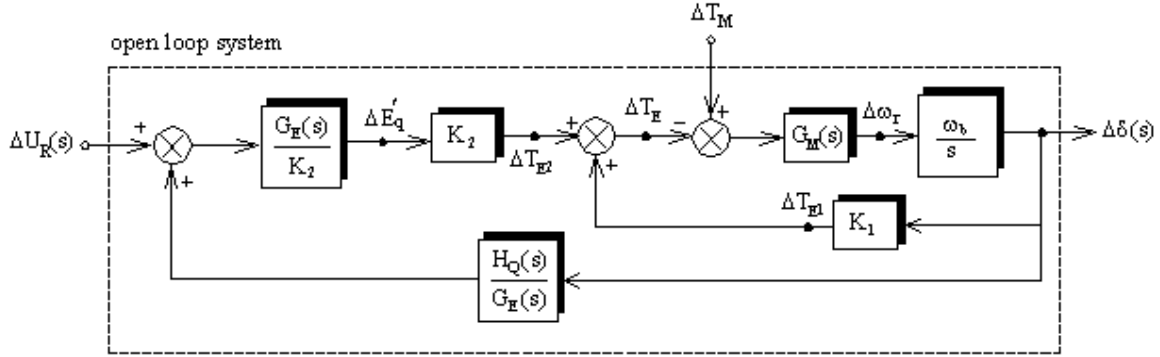


Fig. 7. Transfer function block diagram of SMIB power system.

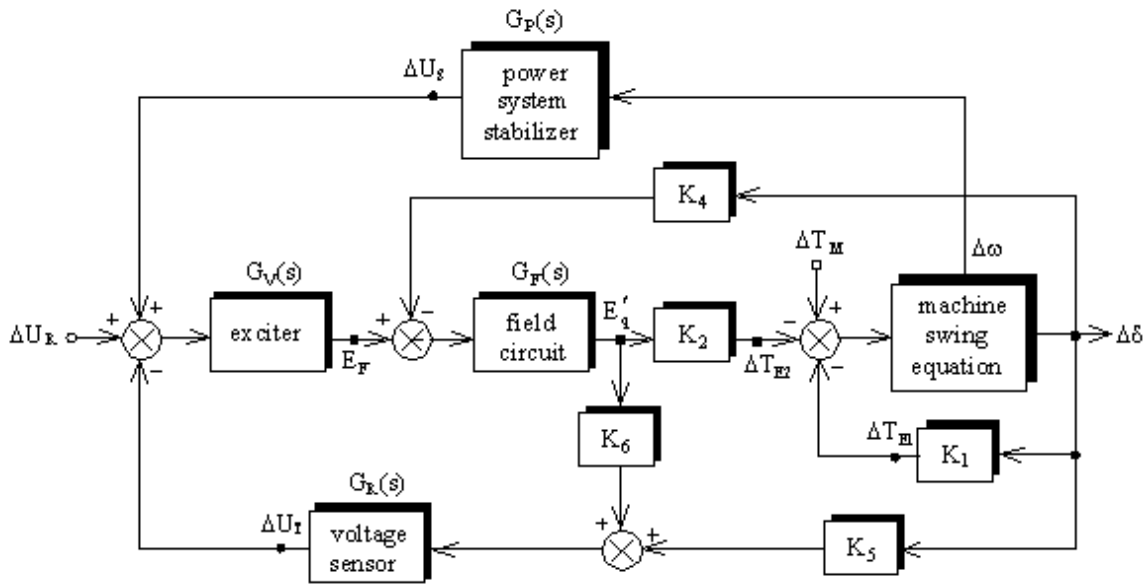


Fig. 8. Single-machine infinite-bus model.

where the coefficients h_0 through h_6 are given by:

$$h_6 = g_5 + \frac{1}{T_W} \quad (17)$$

$$h_5 = g_4 + \frac{g_5}{T_W} \quad (18)$$

$$h_4 = g_3 + \frac{g_4}{T_W} - K_O K_G K_D \quad (19)$$

$$h_3 = g_2 + \frac{g_3}{T_W} - \frac{K_O K_G}{T_S} (K_P T_S + K_D) \quad (20)$$

$$h_2 = g_1 + \frac{g_2}{T_W} - \frac{K_O K_G}{T_S} (K_P + K_I T_S) \quad (21)$$

$$h_1 = g_0 + \frac{g_1}{T_W} - \frac{K_O K_G K_I}{T_S} \quad (22)$$

$$h_0 = \frac{g_0}{T_W} \quad (23)$$

To increase the system damping, the eigenvalue-based objective function is considered as follows:

$$J = \max[\text{Real}(\lambda_i)] \quad (24)$$

where λ_i is the i th electromechanical mode eigenvalue. In the optimization process, it is aimed to minimize J in order to shift the poorly damped eigenvalues to the left in s -plane.

4. SIMULATION RESULTS

The nominal operating conditions and system parameters are given in Table 1. The optimal gains of the PI-PSS and PID-PSS are shown in Table 2. The K_I value under normal load operation is 1.4462, therefore the electromechanical mode natural angular frequency (ω_n) is 10.7448 rad/s. The system eigenvalues with and without the proposed

Table 1. System parameters and operation data.

Generator	$J_M=4.74$, $X_d=1.7$, $X'_d=0.254$ $X_q=1.64$, $T'_{d0}=5.9$ s, $f=60$ Hz
IEEE type-ST1 excitation system	$K_A=400$, $T_A=0.05$ s
IEEE type-DC1 excitation system	$K_A=400$, $T_A=0.05$ s, $K_E=-0.17$ $T_E=0.95$ s, $K_S=0.025$, $T_S=1$ s
Normal load operation	$P_{EO}=1$, $Q_{EO}=0.62$, $U_{TO}=1.172$
Heavy load operation	$P_{EO}=1.4$, $Q_{EO}=1.1$, $U_{TO}=1.172$
Light load operation	$P_{EO}=0.3$, $Q_{EO}=0.1$, $U_{TO}=1.172$
Transmission line reactance	$R_E=0.02$, $X_E=0.4$
Undamped natural angular frequency	$\omega_n=10.7448$ rad/s

Table 2. System parameters and operation data.

PSS	Parameters
PID-PSS	$T_W=0.1149$ s, $K_G=20$, $K_P=-0.6871$, $K_I=-7.9162$, $K_D=0.0688$
PI-PSS	$T_W=0.1$ s, $K_G=10$, $K_P=-1.075$, $K_I=-15.528$

Table 3. System eigenvalues for normal load operation.

Without PSS	With PID-PSS
-0.2350±j10.7852	-2.7130±j10.8539
-8.1340±j8.9851	-7.8708±j3.6719
-3.0830	-3.7595±j6.3345
-1.5520	-1.3896
---	0
---	---

Table 4. System eigenvalues for heavy load operation.

Without PSS	With PID-PSS
-0.301±j10.1575	-4.0471±j10.6330
-7.7731±j9.3124	-1.6751±j7.2454
-4.3901	-8.6648±j3.2515
-1.3762	-1.3020
---	0
---	---

Table 5. System eigenvalues for high load operation.

Without PSS	With PID-PSS
-0.3712±j8.7370	-1.4517±j6.8385
-7.6502±j8.6151	-5.1094±j8.9276
-4.0019	-7.8385±j2.7312
-1.3282	-1.2769
---	0
---	---

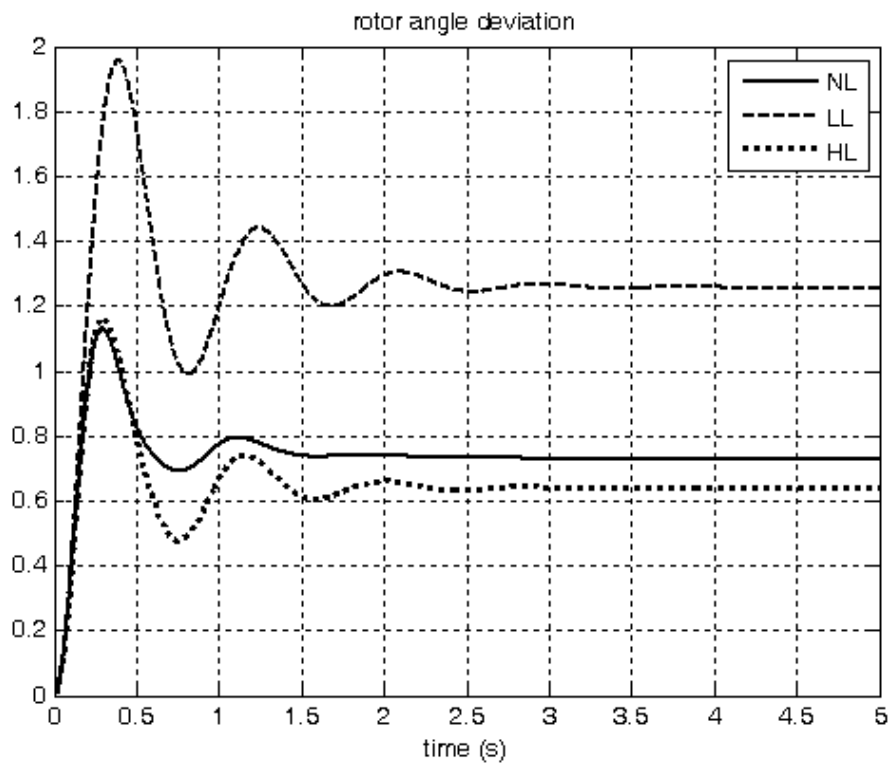
stabilizer for three different conditions are given in Tables 3, 4 and 5.

It shows the electrometrical mode eigenvalue with its damping ratio for the open loop system.

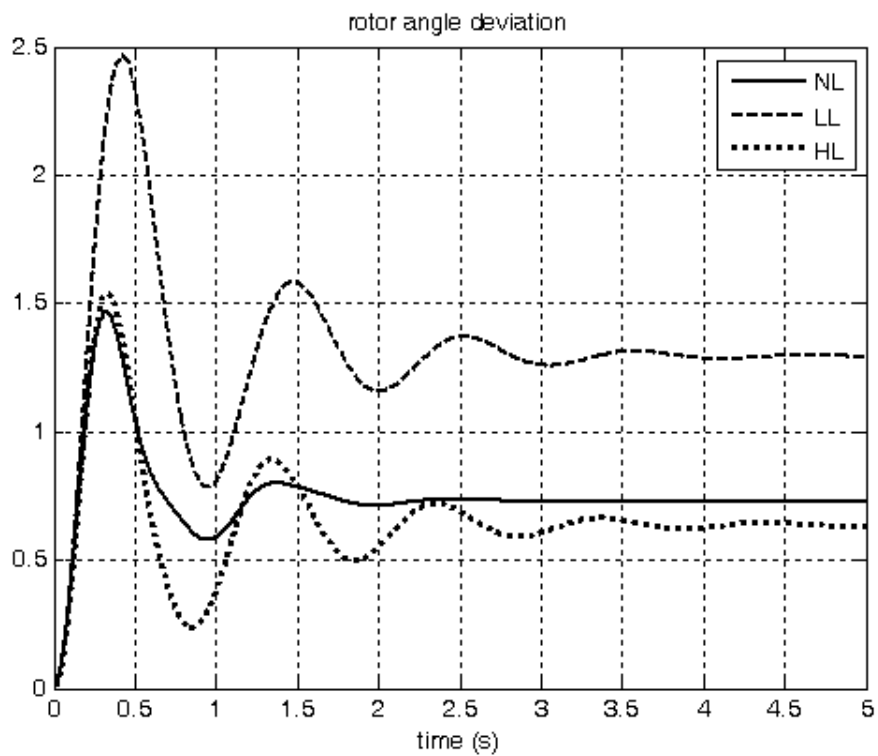
Also, it is observed that the electromechanical mode for the open-loop system, which are characterized by the eigenvalues $-0.2350 \pm j 10.7852$ for normal operating, $-1.8391 \pm j 7.4204$ for heavy load and $-1.6506 \pm j 7.3189$ for light load, are poorly damped.

It is clear that the system stability is greatly enhanced with the proposed stabilizers. The system response without applying any PSS is more oscillatory in heavy load condition. The dynamic behavior response of the SMIB power system as the function of the loading is shown in Figs. 9 and 10. In all the figures, the response with

normal load is shown with dotted line with legend NL, the response with light load is shown with dashed lines with legend LL and the response with heavy load is shown with solid line with legend HL respectively. Table 6 shows the summary of the system dynamic characteristics such as settling time (t_s), peak time (t_p) and overshoot percentage (M_p). The system responses are shown in Fig. 11. In the figures, the response without any PSS is shown with dotted line with legend NP, the response with conventionally designed power system stabilizer is shown with dashed lines with legend CP and the response with proposed PID-PSS is shown with solid line with legend PP respectively. As is observed from the figure, the system response for the PID-PSS is optimum in different condition.

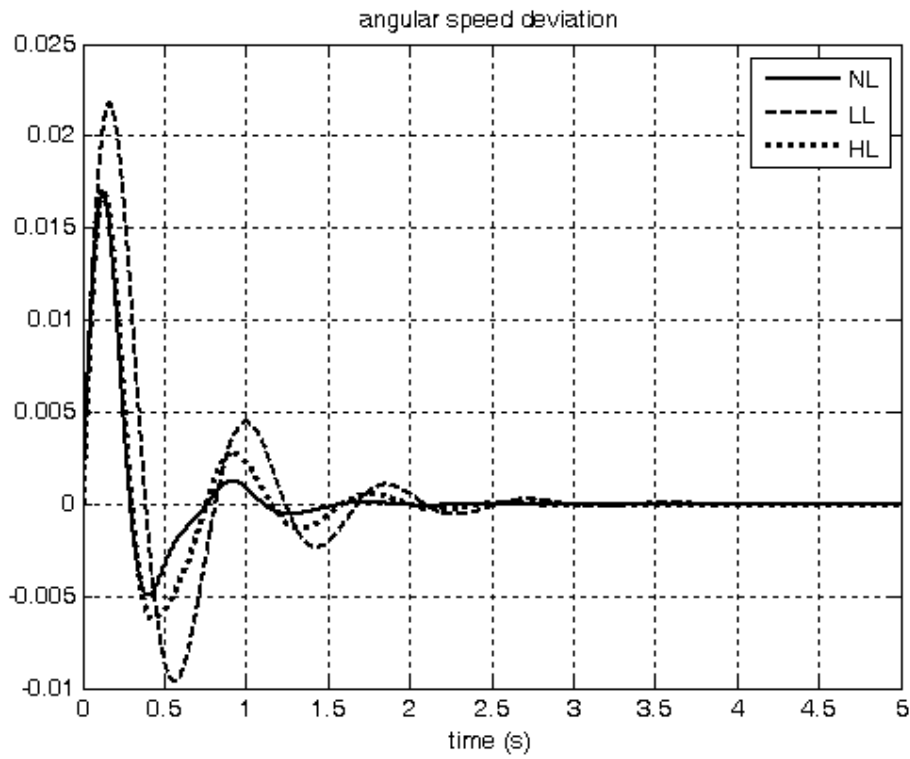


(a) with CPSS

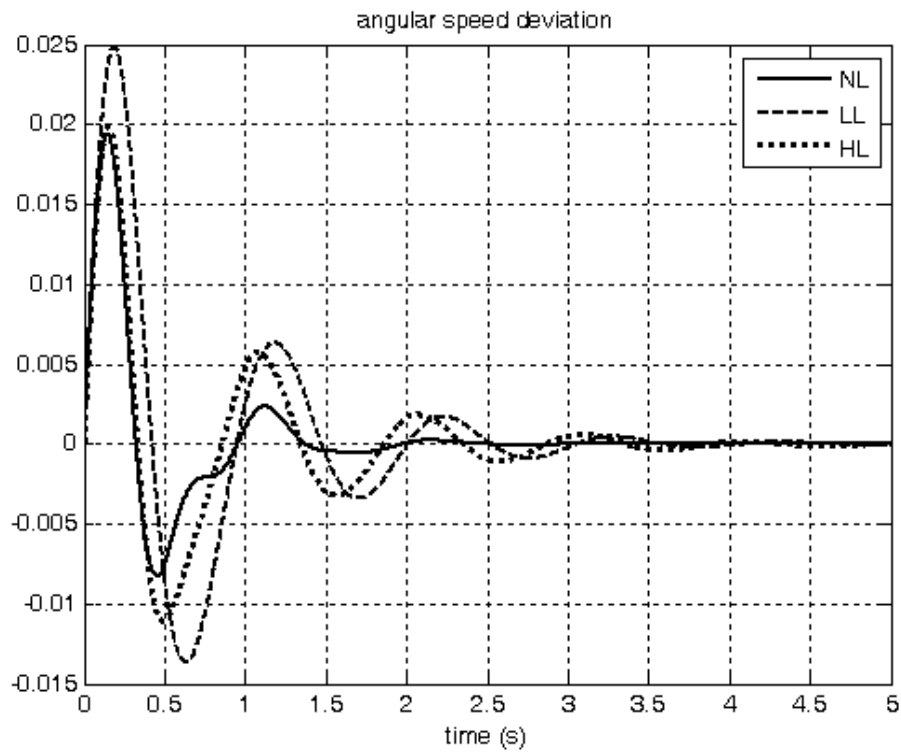


(b) with PID-PSS

Fig. 9. System rotor angle deviation response for different loading.

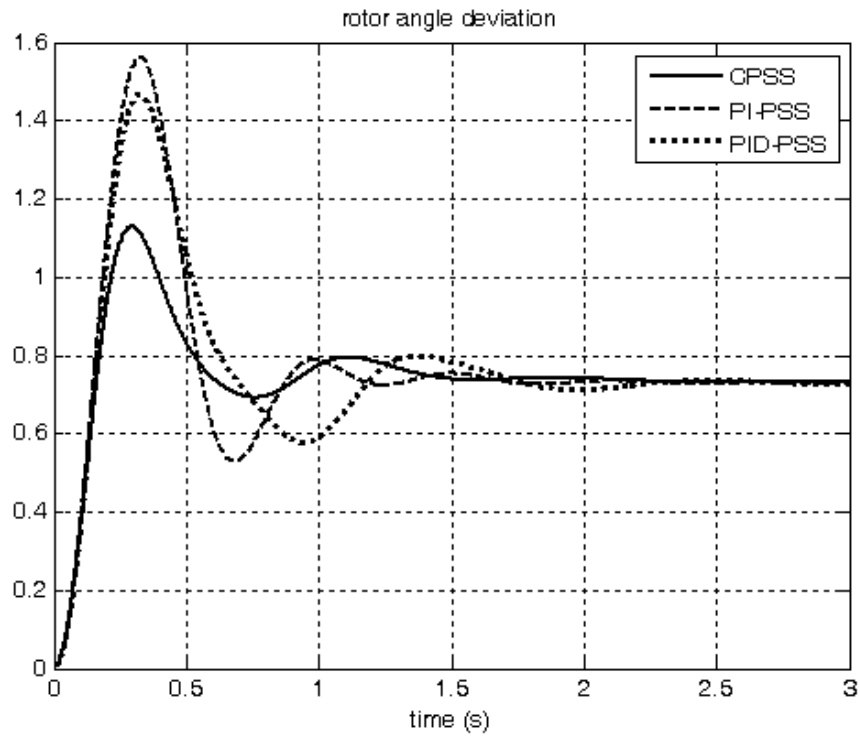


(a) with CPSS

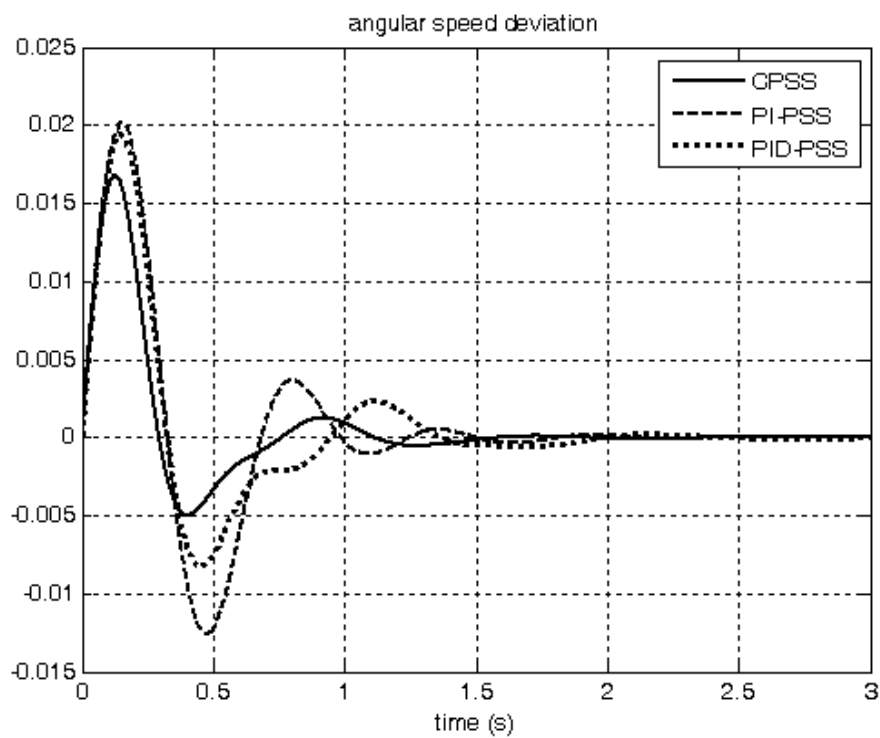


(b) with PID-PSS

Fig. 10. System angular speed deviation response for different loading.



(a) rotor angle deviation



(b) rotor speed deviation

Fig. 11. System dynamic behaviour response with PSS in normal load.

The CPSS has a well-damped response and a lower peak off-shoot in all investigated cases. The damping ratio of the electrometrical mode eigenvalue for different loading of the power system without PSS and with PSS is shown in Table 7. In Fig. 12 the trajectory of the load angle of the generator is

shown. It can be seen that CPSS damping is bigger than PID-PSS and PI-PSS damping. The PSS output response to step mechanical torque change is shown in Fig. 13. As it seems PID-PSS and PI-PSS outputs are better than the CPSS output.

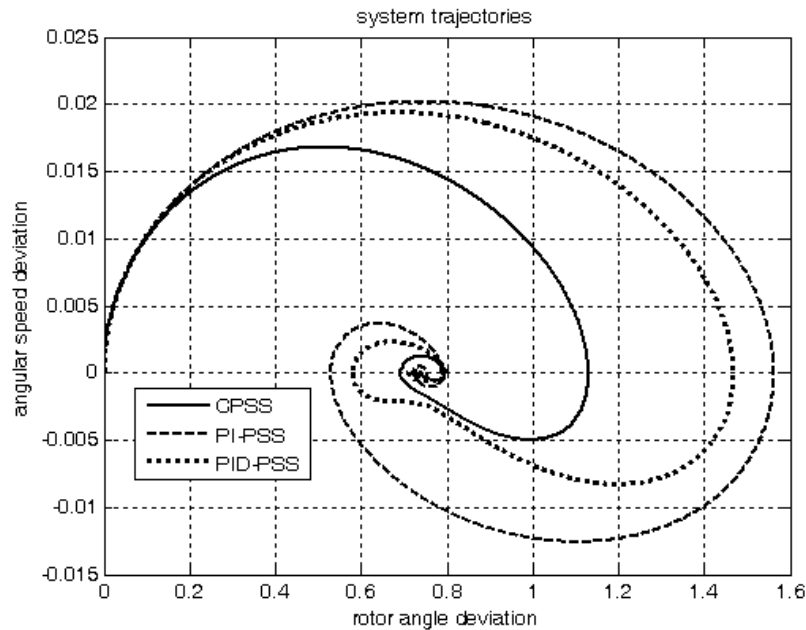


Fig. 12. System trajectories in the δ - ω phase-plane of the generator.

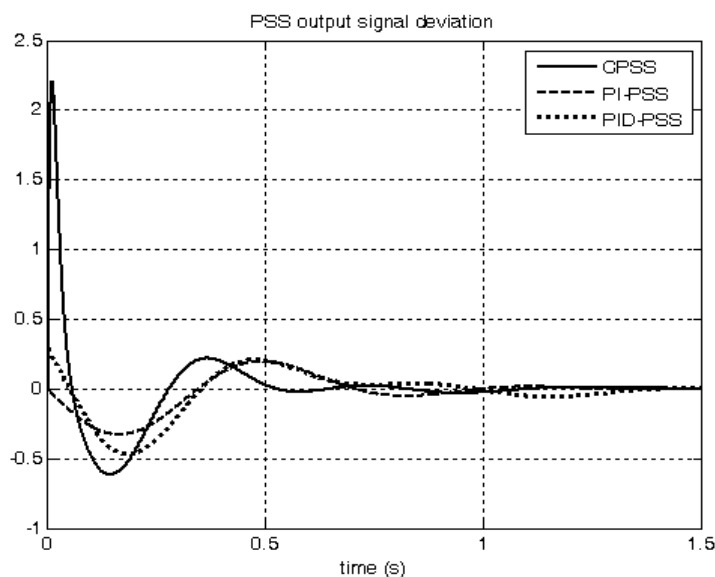


Fig. 13. PSS output response to a step mechanical torque change.

Table 6. System dynamic characteristics.

Loading	With PI-PSS			With PID-PSS		
	t_s	t_p	MP%	t_s	t_p	MP%
Normal loading	1.7 s	3 s	55.21	1.50 s	0.32 s	101.68
Heavy loading	2.5 s	0.3	82.28	3.50 s	0.33 s	142.81
Light loading	3 s	0.4 s	55.85	3.54 s	0.42 s	90.95

Table 7. Damping rate.

Loading	Without PSS	PI-PSS	PID-PSS
Normal loading	0.0218	0.2787	0.2425
Heavy loading	0.0030	0.2406	0.2253
Light loading	0.0424	0.2200	0.2077

5. CONCLUSION

PSS is a control system applied to the generator which sends the appropriate control signals to the voltage regulator to damp the oscillation of the system. A comparison between three different power system stabilizers (CPSS, PI-PSS and PID-PSS) has been carried out on a SMIB power system. Time domain simulations of the system with PID-PSS presented a good speed deviation and change in rotor angle response at different type of loading condition. Simulation results and eigenvalue analysis prove that the CPSS can give adequate performance, although the system-order with CPSS is 9 but the system-order with PID-PSS is 8.

The small signal analysis of the system is investigated based on the transfer functions and the stabilizer parameters are determined based on the transfer function of the system.

A third-order excitation system is also considered.

REFERENCES

- [1] E.L. Miotto, P.B. Araujo, E.V. Fortes, B.R. Gamino, L.F.B. Martins, "Coordinated tuning of the parameters of PSS and POD controllers using bioinspired algorithms", IEEE Trans. on Industry Applications, vol. 54, no. 4, pp. 3845-3857, July-Aug. 2018.
- [2] G. Shahgholian, J. Faiz, "Coordinated control of power system stabilizer and FACTS devices for dynamic performance enhancement- State of art ", Proceeding of the IEEE/IEPS, pp. 1-6, Kyiv, Ukraine, June 2016.
- [3] A. Shoulaie, M. Bayati-Poudeh, G. Shahgholian, "Damping torsional torques in turbine-generator shaft by

- novel PSS based on genetic algorithm and fuzzy logic”, *Journal of Intelligent Procedures in Electrical Technology*, vol. 1, no. 2, pp. 3-10, Sept. 2010.
- [4] G. Shahgholian, M. Maghsoodi, A. Movahedi, “Fuzzy proportional integral controller design for thyristor controlled series capacitor and power system stabilizer to improve power system stability”, *Revue Roumaine des Sciences Techniques*, vol. 61, no. 4, pp. 418-423, 2016.
- [5] O. Kahouli, M. Jebali, B. Alshammari, H.H. Abdallah, "PSS design for damping low-frequency oscillations in a multi-machine power system with penetration of renewable power generations", *IET Renewable Power Generation*, Vol. 13, No. 1, pp. 116-127, Jan. 2019.
- [6] A. Abedini, G. Shahgholian, B. Fani, “Power system dynamic stability improvement using PSS equipped with microcontroller”, *International Journal of Smart Electrical Engineering*, vol. 10m no. 2, pp. 67-76, Spring 2021.
- [7] S. Ghosh, Y.J. Isbeih, M.S. El Moursi, E.F. El-Saadany, "Cross-gramian model reduction approach for tuning power system stabilizers in large power networks", *IEEE Trans. on Power Systems*, vol. 35, no. 3, pp. 1911-1922, May 2020.
- [8] G. Shahgholian, A. Rajabi, B. Karimi, “Analysis and design of PSS for multi-machine power system based on sliding mode control theory”, *International Review of Electrical Engineering*, vol. 4, no. 2, Oct. 2010.
- [9] A. Kazemi-Zahrani, M. Parastegari, “Designing PSS and SVC Parameters simultaneously through the improved quantum algorithm in the multi-machine power system”, *Journal of Intelligent Procedures in Electrical Technology*, vol. 8, no. 31, pp. 68-75, Dec. 2017.
- [10] G. Shahgholian, S. Fazeli-Nejad, M. Moazzami, M. Mahdavian, M. Azadeh, M. Janghorbani, S. Farazpey, "Power system oscillations damping by optimal coordinated design between PSS and STATCOM using PSO and ABC algorithms", *Proceeding of the IEEE/ECTI-CON*, Chiang Mai, Thailand, pp. 1-6, July 2016.
- [11] J. Bhukya, V. Mahajan, "Optimization of damping controller for PSS and SSSC to improve stability of interconnected system with DFIG based wind farm", *International Journal of Electrical Power and Energy Systems*, Vol. 108, pp. 314-335, June 2019.
- [12] G. Shahgholian, "Power system stabilizer application for load frequency control in hydro-electric power plant", *Engineering Mathematics*, Vol. 2, No. 1, pp. 21-30, Feb. 2017.
- [13] A. Zamani, S. Kargar Dehnavi, “Compensation of actuator’s saturation by using fuzzy logic and imperialist competitive algorithm in a system with PID controller”, *Journal of Intelligent Procedures in Electrical Technology*, vol. 3, no. 11, pp. 21-26, Sept. 2013.
- [14] R. Shahedi, K. Sabahi, M. Tayana, A. Hajizadeh, “Self-tuning fuzzy PID controller for load frequency control in

- ac micro-grid with considering of input delay”, Journal of Intelligent Procedures in Electrical Technology, Vol. 9, No. 35, pp. 19-26, Dec. 2019.
- [15] W. Chi-Jui, H. Yuan-Yih, "Design of self-tuning PID power system stabilizer for multimachine power systems", IEEE Trans. on Power Systems, vol. 3, no. 3, pp. 1059-1064, Aug. 1988.
- [16] H. Alkhatib, J. Duveau, "Robust design of power system stabilizers using adaptive genetic algorithms", World Academy of Science, Engineering and Technology, pp. 267-272, vol. 64, May 2010.
- [17] L. Chaib, A. Choucha, S. Arif, "Optimal design and tuning of novel fractional order PID power system stabilizer using a new metaheuristic Bat algorithm", Ain Shams Engineering Journal, vol. 8, no. 2, pp. 113-125, June 2017.
- [18] P.K. Ray, S.R. Paital, A. Mohanty, Y.S.E. Foo, A. Krishnan, H.B. Gooi, G.A. J. Amaratunga, "A hybrid firefly-swarm optimized fractional order interval type-2 fuzzy PID-PSS for transient stability improvement", IEEE Trans. on Industry Applications, vol. 55, no. 6, pp. 6486-6498, Nov.-Dec. 2019.
- [19] A.S.V Vijaya Lakshmi, R.R. Manyala, S.K. Mangipudi, "Design of a robust PID-PSS for an uncertain power system with simplified stability conditions", Protection and Control of Modern Power Systems, vol. 5, , no. 20, pp. 1-16, 2020.
- [20] M. Mahdavian, A. Movahedi, G. Shahgholian, M. Janghorbani, "Coordinated control of PSS and variable impedance devices by using AVURPSO to enhance the stability in power system", Proceeding of the IEEE/ECTICON, pp. 407-410, Phuket, Thailand, June 2017.
- [21] G. Shahgholian, A. Rajabi, B. Karimi, M. Yousefi, "Design of power system stabilizer based on sliding mode control theory for multi-machine power system", Journal of Intelligent Procedures in Electrical Technology, vol. 1, no. 1, pp. 13-22, March 2010.
- [22] S. Jalali, G. Shahgholian, "Designing of power system stabilizer based on the root locus method with lead-lag controller and comparing it with PI controller in multi-machine power system", Journal of Power Technologies, vol. 98, no. 1, pp. 45-56, March 2018.
- [23] K. Bhattacharya, J. Nanda, M.L. Kothari, "Optimization and performance analysis of conventional power system stabilizers", Int. J. of Elec. Pow. and Ene. Sys., Vol.19, No.7, pp. 449-458, Oct. 1997.
- [24] N. Hosaeinzadeh, A. Kalam, "A direct adaptive fuzzy power system stabilizer", IEEE Tran. on Energy Conversion, Vol. 14, No. 4, pp. 1564-1571, Dec. 1999.
- [25] A. Fattollahi, G. Shahgholian, B. Fani, "Decentralized synergistic control of multi-machine power system using power system stabilizer", Signal Processing and Renewable Energy, vol. 4, no. 4, pp. 1-21, Autumn 2020.
- [26] A. Fattollahi, "Simultaneous design

- and simulation of synergetic power system stabilizers and a thyristor-controller series capacitor in multi-machine power systems”, *Journal of Intelligent Procedures in Electrical Technology*, vol. 8, no. 30, pp. 3-14, Sept. 2017.
- [27] C. Osinski, G. Villar Leandro, G.H. da Costa Oliveira, "Fuzzy PID controller design for LFC in electric power systems", *IEEE Latin America Transactions*, vol. 17, no. 01, pp. 147-154, Jan. 2019.
- [28] M. Lotfi-Forushani, B. Karimi, G. Shahgholian, “Optimal PID controller tuning for multivariable aircraft longitudinal autopilot based on particle swarm optimization algorithm”, *Journal of Intelligent Procedures in Electrical Technology*, vol. 3, no. 9, pp. 41-50, June 2012.
- [29] L. Shen, H. Xiao, "Delay-dependent robust stability analysis of power systems with PID controller", *Chinese Journal of Electrical Engineering*, vol. 5, no. 2, pp. 79-86, June 2019.
- [30] T. Chaiyatham, I. Ngamroo, "Improvement of Power System Transient Stability by PV farm with fuzzy gain scheduling of PID controller", *IEEE Systems Journal*, vol. 11, no. 3, pp. 1684-1691, Sept. 2017.
- [31] M. Mahdavian, G. Shahgholian, M. Janghorbani, S. Farazpey and M. Azadeh, "Analysis and simulation of PID-PSS design for power system stability improvement", *Proceeding of the IEEE/ECTI-CON*, pp. 1-6, Chiang Mai, Thailand, June/July 2016.